


Determination of length distribution of TEMPO-oxidized cellulose nanofibrils by field-flow fractionation/multi-angle laser-light scattering analysis

Ryoya Hiraoki · Reina Tanaka  · Yuko Ono · Masahide Nakamura · Takuya Isogai · Tsuguyuki Saito  · Akira Isogai 

Received: 9 October 2017 / Accepted: 22 January 2018 / Published online: 25 January 2018
© Springer Science+Business Media B.V., part of Springer Nature 2018

Abstract Aqueous nanocellulose dispersions were prepared from wood cellulose by 2,2,6,6-tetramethylpiperidine-1-oxyl radical (TEMPO)-mediated oxidation. The obtained TEMPO-oxidized cellulose was converted into TEMPO-oxidized cellulose nanofibrils (TOCNs) of different lengths by controlling the nanofibrillation conditions in water or using dilute acid hydrolysis. The average lengths and length distributions of TOCNs have been measured from transmission electron microscopy (TEM) and atomic force microscopy (AFM) images. However, because the number of nanocelluloses observable in TEM and AFM images is limited, a more reliable method is needed to obtain the lengths/length distributions of TOCNs. In this study, the aqueous TOCN dispersions were subjected to a combination of field-flow fractionation (FFF) and multi-angle laser-light scattering (MALLS). The optimum FFF operation conditions for the acid-hydrolyzed TOCN were first established to obtain reasonable data. For TOCNs with average lengths > 400 nm, suitable separation could not be achieved using the FFF/MALLS system. In contrast, the TOCNs with average

lengths of 170 and 270 nm were adequately separated according to their sizes by the FFF system. The TOCN length distribution patterns corresponded well to those obtained from TEM images. However, the amounts of TOCNs with lengths > 250 nm were underestimated compared with those determined from TEM images. For TOCNs with average lengths of 170 and 270 nm, the molar mass at each TOCN length was determined using the FFF/MALLS system combined with a refractive index detector, where a specific refractive index increment of 0.165 mL/g was used for TOCN.

Keywords TEMPO-oxidized cellulose nanofibril · Length distribution · Field-flow fractionation · Multi-angle laser-light scattering · Acid-hydrolyzed TEMPO-oxidized cellulose nanofibril

Introduction

The morphologies of nanocelluloses primarily and intrinsically govern the mechanical, optical, thermal, oxygen-barrier, and other fundamental properties of nanocellulose bulk materials and nanocellulose-containing composite materials (Eichhorn et al. 2009; Habibi et al. 2010; Klemm et al. 2011; Moon et al. 2011). Therefore, the establishment of accurate determination/controlling methods for the width/width distribution and length/length distribution of

R. Hiraoki · R. Tanaka · Y. Ono · T. Isogai · T. Saito · A. Isogai (✉)
Department of Biomaterial Sciences, The University of Tokyo, Bunkyo-ku, Tokyo 113-8657, Japan
e-mail: aisogai@mail.ecc.u-tokyo.ac.jp

M. Nakamura
Shoko Science, 2-4-1 Shibakouen, Minato-ku, Tokyo 105-8432, Japan

nanocelluloses is essential for the expansion of their applications to commodity and high-tech material fields. Because most nanocelluloses are prepared by mechanical disintegration of cellulose in water, they have heterogeneous morphologies in terms of width and length and form complicated network structures (Isogai 2013). It is, thus, difficult to scientifically and accurately determine their widths/width distributions and lengths/length distributions.

In contrast, cellulose nanocrystals (CNCs) prepared from plant celluloses by acid hydrolysis using, for instance, 64% H₂SO₄, 2,2,6,6-tetramethylpiperidine-1-oxyl radical (TEMPO)-oxidized cellulose nanofibrils (TOCNs) and phosphorylated cellulose nanofibrils (PhCNs) are individually nano-dispersed in water without the formation of any network structures under appropriate preparation conditions (Habibi et al. 2010; Isogai et al. 2011; Klemm et al. 2011; Noguchi et al. 2017). Therefore, their widths/width distributions and lengths/length distributions are more likely to be accurately measured than those of nanocelluloses forming complicated network structures in water.

The average lengths and length distributions of nanocelluloses have been measured primarily from transmission electron microscopy (TEM) and atomic force microscopy (AFM) images, where 100–300 nanocelluloses are counted for length/length distribution measurements (Elazzouzi-Hafraoui et al. 2008; Kontturi and Vuorinen 2009; Lahiji et al. 2010; Shinoda et al. 2012). However, because the number of nanocelluloses observable in TEM and AFM images is limited, a more reliable method is needed to obtain the lengths/length distributions of CNCs, TOCNs, and PhCNs. Tanaka et al. (2014, 2015) reported methods to determine the average lengths of TOCNs from the shear and intrinsic viscosities of dilute TOCN/water dispersions. In particular, an empirical equation relating the intrinsic viscosities of TOCN/water dispersions to the average aspect ratios of the TOCNs was proposed based on various experimental data. This equation is applicable to TOCNs with various lengths, widths, and rigidities (from rigid rods to flexible fibrils) (Tanaka et al. 2015). Because the length determination method using intrinsic viscosities covers more than 10¹⁰ TOCN elements, more reliable data can be obtained than with the TEM or AFM method, where only 100–300 TOCN elements are measured.

However, the method using intrinsic viscosities only provides one average length value for one TOCN

sample, and length distributions cannot be obtained. Because TOCNs have wide length distributions (Tanaka et al. 2015) depending on the preparation conditions, the development of a simple and reliable method to determine length distributions is critical. Field-flow fractionation (FFF) has been applied to separation and analyses of synthetic and natural polymer molecules dissolved in water, latex particles, carbon nanotubes, and other nanoparticles and nanorods dispersed in water (Chun et al. 2008; Messaud et al. 2009; Wyatt 2014). The molecules and particles separated by the FFF system are analyzed by multi-angle laser-light scattering (MALLS) to determine their sizes and size distributions. Details of the separation principles, approximation conditions, and limitations of FFF/MALLS for determination of the length distribution of CNCs have been previously reported (de Souza Lima and Borsali 2002, 2004; Gimbert et al. 2003; Braun et al. 2008; Guan et al. 2012).

The length distributions of CNCs have been analyzed by FFF/MALLS, and their length distributions were determined under various operation conditions. The results were consistent with those obtained from TEM images (de Souza Lima and Borsali 2002; Guan et al. 2012). However, the morphologies and surface charges of CNCs are significantly intrinsically different from those of TOCNs, which have abundant anionically charged sodium carboxylate groups on their surfaces. Therefore, in this study, we prepared four TOCNs with different average lengths and applied FFF/MALLS to determine their length distributions.

Experimental

Materials

A never-dried softwood bleached kraft pulp (SBKP) (Nippon Paper Industries Co. Ltd., Tokyo, Japan) with water content of 80% was used as the starting wood cellulose. Other laboratory-grade chemicals and solvents were used without further purification (Wako Pure Chemicals, Tokyo, Japan).

Preparation of TOCN dispersion

A fibrous TEMPO-oxidized cellulose was prepared from SBKP using a TEMPO/NaBr/NaClO system in water at pH 10 for 5 h followed by successive washing

with water using centrifugation. The TEMPO-oxidized cellulose was further oxidized with NaClO_2 in water at pH 4.8 for 2 day to convert a small amount of the C6-aldehyde groups present in the oxidized cellulose into C6-carboxylate groups (Shinoda et al. 2012; Tanaka et al. 2014). The carboxylate content of the TEMPO-oxidized cellulose was ~ 1.3 mmol/g. The TEMPO-oxidized cellulose/water suspension (0.1%, w/v) was sonicated for 10, 40, and 80 min (Tanaka et al. 2015) to prepare three TOCN/water dispersions with different particle lengths: TOCN-10, TOCN-40, and TOCN-80, respectively. The TEMPO-oxidized cellulose was acid-hydrolyzed in 2.5 M HCl at 105 °C for 4 h, followed by washing thoroughly with water using centrifugation. The acid-hydrolyzed TEMPO-oxidized cellulose/water suspension (0.3%, w/v) was sonicated for 10 min to prepare acid-hydrolyzed TOCN (AH-TOCN) (Tanaka et al. 2015). The length-weighted average lengths of the AH-TOCN and TOCN-80 were 170 and 270, respectively, as determined from TEM images (Tanaka et al. 2014, 2015). The sample preparation and operation conditions for the TEM and AFM observations are described elsewhere (Tanaka et al. 2014, 2015).

FFF/MALLS analysis

The concentration of all the TOCN/water dispersions for FFF/MALLS analysis was adjusted to 0.1% (w/v). Fractionation of the TOCNs and determination of the corresponding lengths and masses were performed using an Eclipse FFF (Wyatt Technology Co., Santa Barbara, USA) and MALLS (DAWN HELEOS II, Wyatt Technology Co.) with an isocratic pump (Agilent 1200, Agilent Technologies, Santa Clara, USA) and vacuum degasser (Gastorr TG-14, Flom Inc., Tokyo, Japan) (Guan et al. 2012). The 0.05 mL TOCN/water dispersion was injected into a FFF separation channel equipped with a polyethersulfone membrane filter with a cut-off molecular mass of 5 kDa. For the eluent, 0–40 mM NaCl was used, and the elution flow rate was fixed at 1.0 mL/min. The cross flow rate varied from 0.1 to 1.5 mL/min and was then ramped down to 0.1 mL/min for 10–80 min to achieve optimum separation conditions. Details concerning the MALLS and differential refractive index detection (RI) systems are described elsewhere (Ono et al. 2016a, b). The refractive indices of the AH-TOCN/water dispersions at concentrations of 0.078, 0.130, 0.275, and 0.550 mg/

mL were determined using an off-line refractive index detector (Optilab T-rEx, Wyatt Technologies), and the specific refractive index increment (dn/dc) was determined to be 0.165 mL/g from the slope of the concentration/refractive index plots (Ono et al. 2016a; Shimizu et al. 2016). The relationships between the FFF elution time and TOCN length or mass values were established by data acquisition and processing using Astra 5 software (Wyatt Technology Co.). The principles of FFF/MALLS analysis used to determine the TOCN length and mass values are described elsewhere (Gimbert et al. 2003; Braun et al. 2008; Guan et al. 2012). Briefly, particles dispersed or molecules dissolved in a solution injected into the FFF channel are separated by a semipermeable ultrafiltration membrane with channel and cross flows of an eluent, according to their sizes. The separated particles or molecules are eluted off with the eluent from the FFF channel, and the particle and molecular size at each elution time is determined with a MALLS detector.

Results and discussion

Optimum NaCl concentration of AH-TOCN dispersion for FFF separation

The optimum NaCl concentration for the eluent in the FFF separation was first evaluated by changing the NaCl concentration from 0 to 40 mM. When ultrapure water was used as the eluent, almost all the AH-TOCN elements were eluted at an elution time of ~ 7 min, and the fibril length plots were scattered as a function of the elution time. Thus, suitable fractionation of TOCNs depending on their sizes could not be achieved in this case (Fig. 1a). Because the AH-TOCN as well as other TOCNs have abundant anionically charged sodium carboxylate groups on their surfaces, the TOCN elements may be fully expanded and their Debye lengths may increase in pure water (Fukuzumi et al. 2014; Tanaka et al. 2014), resulting in the inadequate FFF elution pattern in Fig. 1a. When 40 mM NaCl solution was used, the length plots of the AH-TOCNs increased with increasing elution time, depending on their sizes. However, a shoulder peak most likely caused by partial agglomeration of AH-TOCN elements appeared at ~ 25 min in the FFF elution pattern detected by MALLS (Fig. 1b). In contrast, almost all the TOCN elements were adequately fractionated depending on their sizes when

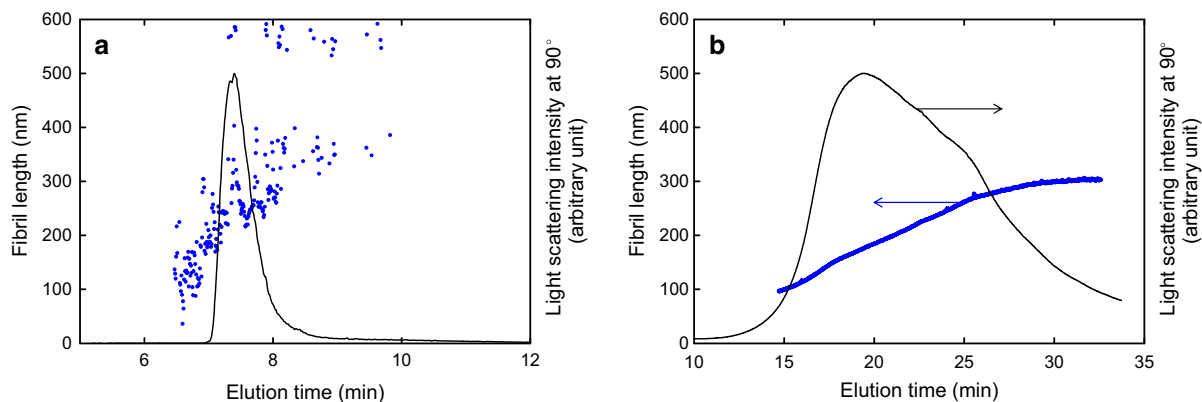


Fig. 1 FFF elution patterns and corresponding length plots determined using MALLS for AH-TOCN with pure water (**a**) and 40 mM NaCl (**b**) as the eluent

5 mM NaCl solution was used as the eluent. Therefore, hereafter, 5 mM NaCl solution was used as the eluent for the FFF/MALLS analysis.

Optimum cross flow rate and gradient time for FFF separation

When a cross flow rate and gradient time of 0.8 mL/min and 80 min, respectively, were used (Guan et al. 2012), an anomalous peak most likely caused by partial agglomeration of AH-TOCN elements was detected. The cross flow rates were then varied from 0.1 to 1.5 mL/min. The corresponding FFF elution patterns revealed some agglomeration of AH-TOCN elements at cross flow rates > 0.5 mL/min. The FFF separation capability slightly decreased at a cross flow rate of < 0.3 mL/min. The optimum cross flow rate was then fixed at 0.4 mL/min. Next, the optimum gradient time was estimated. The FFF separation capability became low for gradient times of 10–20 min. In contrast, the analytical data obtained using MALLS became inaccurate when the gradient time was 60–80 min because of the low AH-TOCN concentration in the eluent. Therefore, the gradient time of 40 min yielded the most reasonable data. In summary, the optimum eluent, cross flow rate, and gradient time for FFF separation of TOCNs were determined to be 5 mM NaCl, 0.4 mL/min, and 40 min, respectively.

Determination of TOCN length distributions by FFF/MALLS

Figure 2a presents the FFF elution pattern and corresponding fibril length plots determined using MALLS

for the AH-TOCN; these data were measured under the optimum conditions determined in the previous section. No peaks caused by TOCN agglomeration were detected in the FFF elution pattern. The fibril length plots increased with increasing elution time up to 40 min, indicating that the TOCNs were adequately separated according to their sizes in this elution time range. Figure 2b presents the results for TOCN-80 measured under the same conditions as those for AH-TOCN. The length-weighted average length of TOCN-80 was 270 nm according to the TEM images. No peak due to TOCN agglomeration was detected in the FFF elution pattern obtained using MALLS, and the fibril length plots increased with increasing elution time up to 42 min.

Figure 2c presents the results for TOCN-40, which had a length-weighted average length > 400 nm. The length plots increased with increasing elution time up to 55 min. However, a shoulder peak was observed at the elution time of 51 min, indicating the presence of TOCN agglomerates. Figure 2d presents the results for TOCN-10, which most likely had the highest length-weighted average length of the TOCNs used in this study. The fibril length plots were almost constant as a function of FFF elution time, indicating that the TOCN-10 elements could not be separated according to their sizes. Thus, TOCN-10 with long fibril lengths cannot be separated using the FFF system under the conditions used in this study. In this study, the samples injected to the FFF system had the same 0.1% (w/v) TOCN or AH-TOCN concentration, and the same 40 mM NaCl was used as the eluent. These conditions may have been unsuitable for the long TOCN-10 elements.

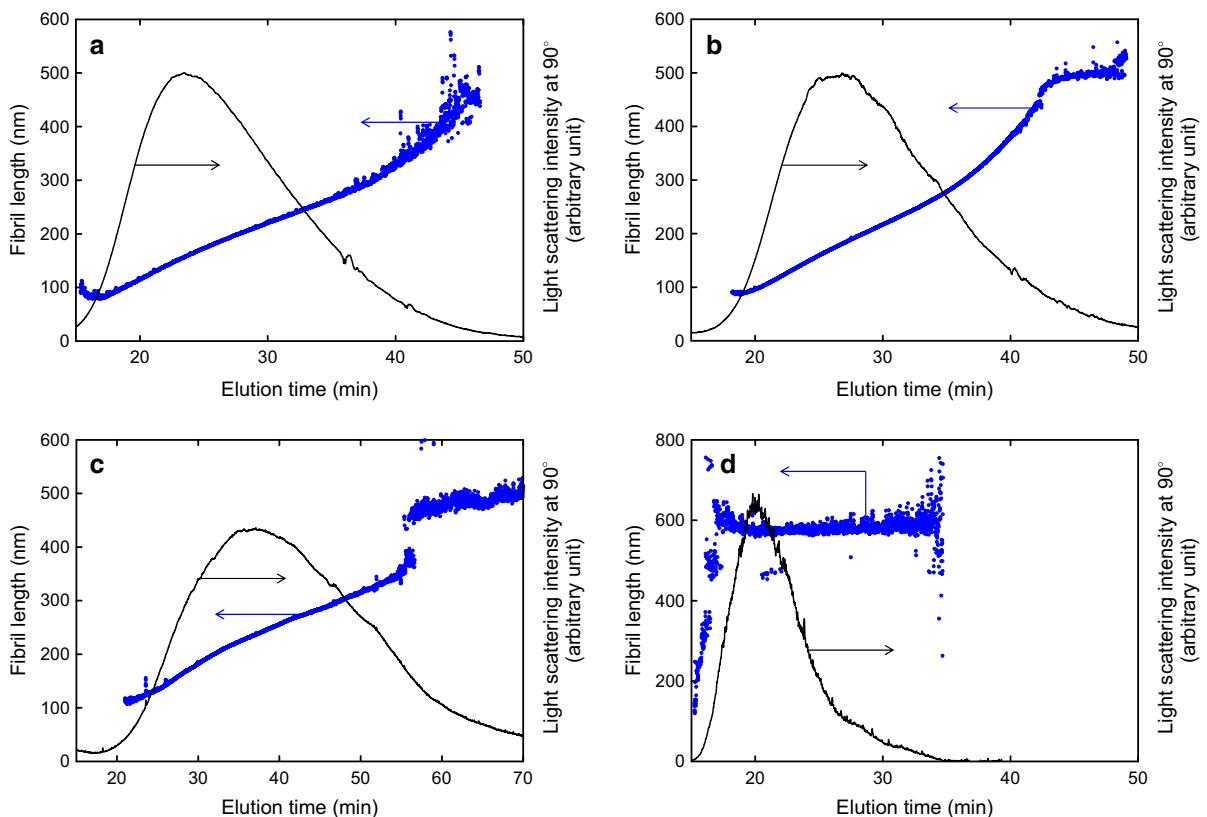


Fig. 2 FFF elution pattern and corresponding length plots determined by MALLS for AH-TOCN (a), TOCN-80 (b), TOCN-40 (c), and TOCN-10 (d)

Consequently, FFF/MALLS analysis for determination of length distributions is limited to TOCNs with length-weighted average lengths < 300 nm under the analytical conditions used in this study.

TOCN length distributions determined by FFF/MALLS and TEM

Figure 3 shows the relationships between the length distribution determined by FFF/MALLS and TEM for AH-TOCN (a) and TOCN-80 (b). The length distribution determined by FFF/MALLS was mostly consistent with that determined from TEM images. Thus, FFF/MALLS is applicable for determining the length distribution of acid-hydrolyzed TOCNs or TOCNs with average lengths < 200 nm.

However, the length distributions for lengths > 250 nm determined by FFF/MALLS were somewhat underestimated compared with those determined from TEM images. The equations to calculate the

length distribution of nanosized particles from FFF/MALLS data are based on rigid rod models (Braun et al. 2008; Guan et al. 2012). Mostly rigid rod morphologies were observed for AH-TOCN in TEM images (Fig. 4), whereas some curved, bent, and long fibrils with some kinks were observed for TOCN-80 (Tanaka et al. 2014, 2015). These long and flexible TOCN elements may have caused the underestimation of their lengths using the rigid-rod-model based FFF/MALLS analysis.

Another possible explanation for the discrepancy at fibril lengths > 250 nm between FFF/MALLS and TEM in Fig. 3 is the validity limitation of the Rayleigh–Gans–Debye (RGD) approximation (Braun et al. 2008; Guan et al. 2012). The detailed limitation and validity of the RGD approximation have been previously described in detail in terms of parameters of the particle refractive indices of eluent and CNCs, their particle sizes, and the wavelength of MALLS (Braun et al. 2008; Guan et al. 2012). It was concluded

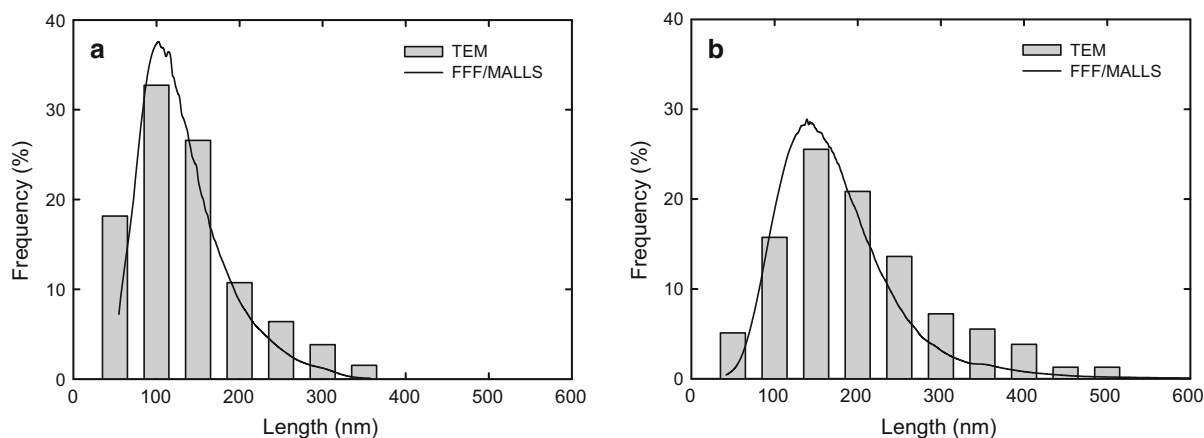


Fig. 3 Length distributions determined using FFF/MALLS and TEM images for AH-TOCN (a) and TOCN-80 (b)

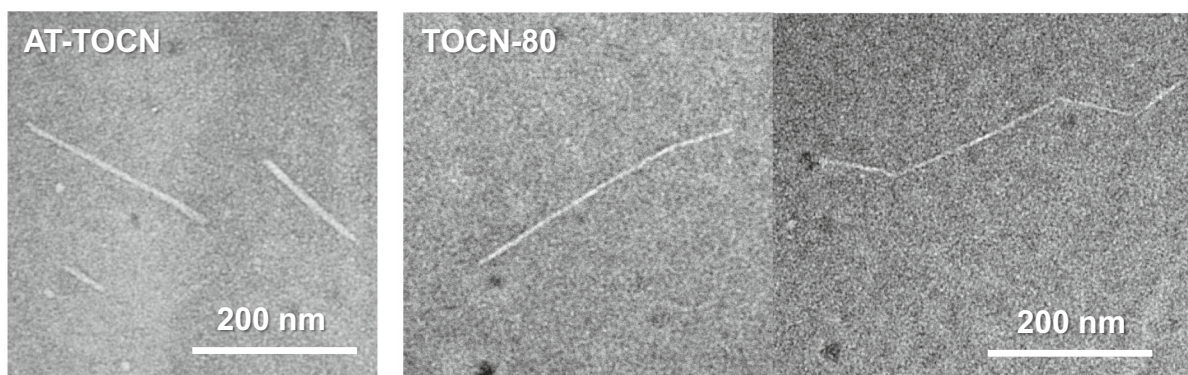


Fig. 4 TEM images of AH-TOCN and TOCN-80

that the RGD approximation cannot be applied to nanocelluloses with lengths > 350 nm. Therefore, it is possible that the length distribution at > 250 nm for AH-TOCN and TOCN-80 cannot be determined quantitatively because of the RGD limitation.

The FFF/MALLS analysis provides more reliable average lengths and length distributions of TOCNs than those determined from TEM images because the FFF/MALLS analysis can cover more than 10^{10} TOCN elements for the length determination when the volume of injected 0.05 mL of 0.1% (w/v) TOCN/dispersions is ~ 50 μ L. In contrast, the lengths of only 200–300 TOCN elements are measured from TEM images. However, the results obtained in this study indicate that only TOCNs with lengths < 300 nm or CNCs provide reasonable lengths and length distributions for the FFF/MALLS analysis.

Determination of TOCN fibril mass by FFF/MALLS

When the dn/dc value of TOCN is used in FFF/MALLS analysis with a RI detector, the fibril mass per mole of TOCN with a particular length can be estimated. Figure 5a presents the FFF elution patterns and corresponding plots of the fibril mass as a function of FFF elution time for AH-TOCN and TOCN-80. Figure 5b shows the relationships between the TOCN fibril length and corresponding fibril mass calculated from the results in Fig. 5b reveal that the mass of AH-TOCN is approximately twice that of TOCN-80 at the same fibril length. The average widths of AH-TOCN and TOCN-80 determined from AFM height images were ~ 3.8 and ~ 2.6 nm, respectively (Tanaka et al. 2015). The FFF/MALLS results in Fig. 5b correspond well to those obtained from AFM images, because the

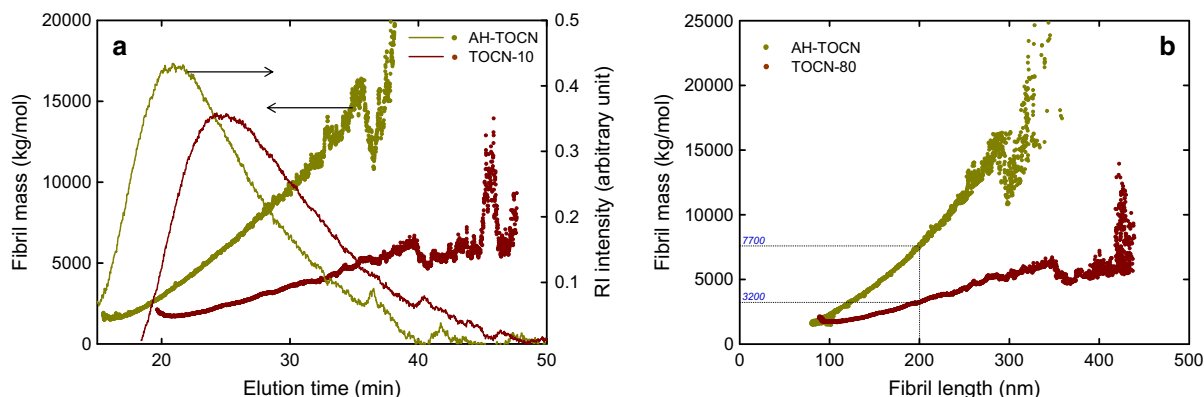


Fig. 5 FFF elution pattern detected by RI and corresponding fibril mass plots for AH-TOCN and TOCN-80 (a), and the relationships between TOCN length and mass values (b)

fibril masses are proportional to the square of the fibril lengths.

The fibril length/mass results in Fig. 5b indicate that the width of one TOCN element increased from ~ 2.6 nm in the original TOCN to ~ 3.8 nm by binding two TOCN elements in a parallel manner. Most likely, the carboxylate-group-containing surface molecules present on each TOCN element were partially degraded and removed from the surface during acid hydrolysis. Then, the TOCN surfaces with almost no carboxylate groups (such as cellulose molecules) agglomerated to form TOCNs with larger widths during acid hydrolysis.

In our previous papers, we assumed that the cross-sections of TOCNs prepared from wood celluloses were square and consisted of $6 \times 6 = 36$ cellulose chains based on TEM and AFM images, and X-ray diffraction (XRD) patterns (Okita et al. 2010; Isogai et al. 2011; Shinoda et al. 2012; Saito et al. 2013). However, Fig. 5b reveals that the TOCN with the fibril length of 200 nm (which corresponds to a degree of polymerization of 400 for the cellulose I crystal) has a ~ 3200 kg/mol. This molar mass value corresponds to the $7 \times 7 = 49$ model, for which the square cross-section of each TOCN consists of cellulose and surface-oxidized cellulose chains. This value is overestimated according to recently published models of cellulose microfibrils in plant cell walls (Cosgrove 2014; Nixon et al. 2016). The molar mass plots of TOCNs swollen in water were determined using FFF/MALLS in this study, different from the fibril widths of TOCNs determined in dry state by TEM, AFM, or XRD. This difference between dry and swollen states

of TOCNs may have caused the difference in fibril widths, because TOCNs have hydrophilic sodium C6-carboxylate groups densely and position-selective present on the surfaces. Further studies are, however, required to clarify the reason for the large cross-sectional TOCN widths, when determined using FFF/MALLS.

Conclusions

The optimum operation conditions of a FFF/MALLS system were established for AH-TOCN and TOCNs, which have abundant anionically charged sodium carboxylate groups on their surfaces. These FFF operation conditions differed from those for CNCs. When AH-TOCN and TOCN-80 with length-weighted average lengths of 170 and 270 nm, respectively, were used, the obtained length distributions were mostly consistent with those determined from TEM images. However, the distributions of lengths > 250 nm determined by FFF/MALLS were underestimated compared with those determined from TEM images. The FFF/MALLS analysis provided no reasonable data for TOCN-40 and TOCN-10 with length-weighted average lengths > 400 nm. Therefore, reliable lengths and length distributions can be obtained by FFF/MALLS analysis only for TOCNs with lengths < 200 nm. The FFF/MALLS/RI analysis also provided fibril mass distributions for AH-TOCN and TOCN-80.

Acknowledgments This research was supported by Core Research for Evolutional Science and Technology (CREST, Grant No. JPMJCR13B2) of the Japan Science and Technology

Agency (JST). We also thank Tiffany Jain, M.S., from Edanz Group (www.edanzediting.com/ac) for editing a draft of this manuscript.

References

- Braun B, Dorgan JR, Chandler JP (2008) Cellulosic nanowhiskers. Theory and application of light scattering from polydisperse spheroids in the Rayleigh–Gans–Debye regime. *Biomacromolecules* 9:1255–1263
- Chun J, Fagan JA, Hobbie EK, Bauer BJ (2008) Size separation of single-wall carbon nanotubes by flow-field flow fractionation. *Anal Chem* 80:2514–2523
- Cosgrove DJ (2014) Re-constructing our models of cellulose and primary cell wall assembly. *Curr Opin Plant Biol* 22:122–131
- de Souza Lima MM, Borsali R (2002) Static and dynamic light scattering from polyelectrolyte microcrystal cellulose. *Langmuir* 18:992–996
- de Souza Lima MM, Borsali R (2004) Rodlike cellulose microcrystals: structure, properties, and applications. *Macromol Rapid Commun* 25:771–787
- Eichhorn SJ, Dufresne A, Aranguren M, Marcovich NE, Capadona JR, Rowan SJ, Weder C, Thielemans W, Roman M, Rennecker S, Gindl W, Veigel S, Keckes J, Yano H, Abe K, Nogi M, Nakagaito AN, Mangalam A, Simonsen J, Benight AS, Bismarck A, Berglund LA, Peijs T (2009) Review: current international research into cellulose nanofibers and nanocomposites. *J Mater Sci* 45:1–33
- Elazzouzi-Hafraoui S, Nishiyama Y, Putaux JL, Heux L, Dubreuil F, Rochas C (2008) The shape and size distribution of crystalline nanoparticles prepared by acid hydrolysis of native cellulose. *Biomacromolecules* 9:57–65
- Fukuzumi H, Tanaka R, Saito T, Isogai A (2014) Dispersion stability and aggregation behavior of TEMPO-oxidized cellulose nanofibrils in water as a function of salt addition. *Cellulose* 21:1553–1559
- Gimbert LJ, Andrew KN, Haygrath PM, Worsford PJ (2003) Environmental applications of flow field-flow fractionation (FIFFF). *Trac Trends Anal Chem* 22:615–633
- Guan X, Cueto R, Russo P, Qi Y, Wu Q (2012) Asymmetric flow field-flow fractionation with multiangle light scattering detection for characterization of cellulose nanocrystals. *Biomacromolecules* 13:2671–2679
- Habibi Y, Lucian L, Rojas OJ (2010) Cellulose nanocrystals: chemistry, self-assembly, and applications. *Chem Rev* 110:3479–3500
- Isogai A (2013) Wood nanocelluloses: fundamentals and applications as new bio-based nanomaterials. *J Wood Sci* 59:449–459
- Isogai A, Saito T, Fukuzumi H (2011) TEMPO-oxidized cellulose nanofibers. *Nanoscale* 3:71–85
- Klemm D, Kramer F, Moritz S, Lindström T, Ankerfors M, Gray D, Dorris A (2011) Nanocelluloses: a new family of nature-based materials. *Angew Chem* 50:5438–5466
- Kontturi E, Vuorinen T (2009) Indirect evidence of supramolecular changes within cellulose microfibrils of chemical pulp fibers upon drying. *Cellulose* 16:65–74
- Lahiji RR, Xu X, Reifenger R, Raman A, Rudie A, Moon RJ (2010) Atomic force microscopy characterization of cellulose nanocrystals. *Langmuir* 26:4480–4488
- Messaud FA, Sanderson RD, Runyon JR, Otte T, Pasch H, Williams SKR (2009) An overview on field-flow fractionation techniques and their applications in the separation and characterization of polymers. *Prog Poly Sci* 34:351–368
- Moon RJ, Martini A, Nairn J, Simonsen J, Youngblood J (2011) Cellulose nanomaterials review: structure, properties and nanocomposites. *Chem Soc Rev* 40:3941–3994
- Nixon BT, Mansouri K, Singh A, Du J, Davis J, Lee JG, Slaubaugh E, Vandavasi VG, O’Neil H, Roberts EM, Roberts AW, Yingling YG, Haigler CH (2016) Comparative structural and computational analysis supports eighteen cellulose synthases in the plant cellulose synthesis complex. *Sci Rep* 6:28696
- Noguchi Y, Homma I, Matsubara Y (2017) Complete nanofibrillation of cellulose prepared by phosphorylation. *Cellulose* 24:1295–1305
- Okita Y, Saito T, Isogai A (2010) Entire surface oxidation of various cellulose microfibrils by TEMPO-mediated oxidation. *Biomacromolecules* 11:1696–1700
- Ono Y, Ishida T, Soeta H, Saito T, Isogai A (2016a) Determination of dn/dc values for cellulose, chitin, cellulose triacetate, and cellobiose dissolved in LiCl/*N,N*-dimethylacetamide. *Biomacromolecules* 17:192–199
- Ono Tanaka R, Funahash R, Takeuchi M, Saito T, Isogai A (2016b) SEC-MALLS analysis of ethylenediamine-pre-treated native celluloses in LiCl/*N,N*-dimethylacetamide: softwood kraft pulp and highly crystalline bacterial, tunicate, and algal celluloses. *Cellulose* 23:1639–1647
- Saito T, Kuramae R, Wohler J, Berglund LA, Isogai A (2013) An ultrastrong nanofibrillar biomaterial: the strength of single cellulose nanofibrils revealed via sonication-induced fragmentation. *Biomacromolecules* 14:248–253
- Shimizu M, Saito T, Nishiyama Y, Iwamoto S, Yano H, Isogai A, Endo T (2016) Fast and robust nanocellulose width estimation using turbidimetry. *Macromol Rapid Commun* 37:1581–1586
- Shinoda R, Saito T, Okita Y, Isogai A (2012) Relationship between length and degree of polymerization of TEMPO-oxidized cellulose nanofibrils. *Biomacromolecules* 13:842–849
- Tanaka R, Saito T, Ishii D, Isogai A (2014) Determination of nanocellulose fibril length by shear viscosity measurement. *Cellulose* 21:1581–1589
- Tanaka R, Saito T, Hondo H, Isogai A (2015) Influence of flexibility and dimensions of nanocelluloses on the flow properties of their aqueous dispersions. *Biomacromolecules* 16:2127–2131
- Wyatt PJ (2014) Measurement of special nanoparticle structures by light scattering. *Anal Chem* 86:7171–7183